

**Quantum three-body Coulomb problem in two dimensions**L. Hilico,<sup>1,2,\*</sup> B. Grémaud,<sup>1</sup> T. Jonckheere,<sup>1,2</sup> N. Billy,<sup>1,2</sup> and D. Delande<sup>1</sup><sup>1</sup>*Laboratoire Kastler Brossel, Université Pierre et Marie Curie, Case 74, 4 Place Jussieu, 75252 Paris, France*<sup>2</sup>*Département de Physique et Modélisation, Université d'Evry Val d'Essonne, Boulevard F. Mitterrand, 91025 Evry cedex, France*

(Received 29 March 2002; published 5 August 2002)

We study the three-body Coulomb problem in two dimensions and show how to calculate very accurately its quantum properties. The use of a convenient set of coordinates makes it possible to write the Schrödinger equation using only annihilation and creation operators of four harmonic oscillators, coupled by various terms of degree up to 12. We analyze in detail the discrete symmetry properties of the eigenstates. The energy levels and eigenstates of the two-dimensional helium atom are obtained numerically, by expanding the Schrödinger equation on a convenient basis set that gives sparse banded matrices, and thus opens up the way to accurate and efficient calculations. We give some very accurate values of the energy levels of the first bound Rydberg series. Using the complex coordinate method, we are also able to calculate energies and widths of doubly excited states, i.e., resonances above the first ionization threshold. For the two-dimensional  $H^-$  ion, only one bound state is found.

DOI: 10.1103/PhysRevA.66.022101

PACS number(s): 03.65.Ge, 31.15.Ar, 31.15.Pf, 71.15.Ap

**I. INTRODUCTION**

Since the very beginning of quantum mechanics, the helium atom has attracted much attention as it is one of the simplest system where the Schrödinger equation cannot be solved exactly. Recently, it has been understood that the lack of an exact solution is the direct quantum counterpart of the nonintegrable character of the corresponding classical dynamics [1]. Indeed, it has been discovered that, for most initial conditions (positions and velocities of the two electrons), the classical dynamics is chaotic, with the total energy and the total angular momentum being the only constants of motion. Together with the development of sophisticated numerical methods for computing the quantum energy levels [2–7], there have been major improvements in semiclassical techniques which allow one to compute approximate values of the energy levels from knowledge of the classical dynamics. The most dramatic success is the use of periodic orbit theory, where the energy levels are calculated from simple properties (action, period, stability, etc.) of a (preferably large) set of classical periodic orbits [1]. Most of the quantum and semiclassical calculations concentrated on states with low total angular momentum for at least two reasons: first, these are the states experimentally prepared when using an optical excitation from a low excited state and, secondly, this is the situation where the classical dynamics is well known.

Of special interest are the  $S$  states with zero total angular momentum. Classically, the motion of the two electrons takes place in a fixed plane. Thus, the classical dynamics is fully identical with the classical dynamics of the two-dimensional (2D) helium atom. It turns out that, although it seems to be a simpler system, there has been only very little interest in this 2D three-body Coulomb problem and essentially no quantum calculation. It is the aim of this paper to fill this hole. It can also be expected that, when a “real” 3D

helium atom with low (or zero) initial momentum is exposed to an external perturbation, its response will not be very different from that of the 2D atom, provided angular momentum does not play a crucial role in the physical processes involved. For example, when a helium atom is exposed to a strong nonresonant low-frequency electromagnetic field, it may absorb a large number of photons leading eventually to single or even double ionization. It seems likely that the correlation between the two electrons plays a major role in this process (especially in the generation of high harmonics of the electromagnetic field), while the total angular momentum remains relatively small. Another example is the production of doubly ionized atoms where a process involving symmetric excitation of the two electrons (with zero total angular momentum) has recently been proposed [8]. In these situations, the full 3D quantum calculation for such a system is not presently feasible, except for the very lowest states. On the other hand, a 2D quantum calculation seems reachable. This would allow one to determine whether the proposed process is relevant or not. It is thus highly desirable to be able to compute accurately the quantum properties of the 2D helium atom.

A second motivation to study the 2D three-body Coulomb problem comes from semiconductor physics. The study of excitons—the bound aggregate of an electron from the conduction band and a hole from the valence band, each particle with a given effective mass—is an important tool to study semiconductors. In 1958, Lampert [9] showed that three-body complexes called triions (an electron or a hole bound to an exciton) should be observable at low temperatures, and this was confirmed later by variational calculations, showing the stability of triions against dissociation into an exciton and a free electron or a hole (see [10] for references). Since then, the progress in semiconductor technology has made possible the fabrication of quasi-2D systems. It was then realized [11,10] that in such systems triions would have an increased stability due to the 2D confinement, and should thus be more easily observable. The triions are responsible for satellites on the excitonic lines in luminescence spectra. Several observa-

\*Electronic address: hilico@spectro.jussieu.fr

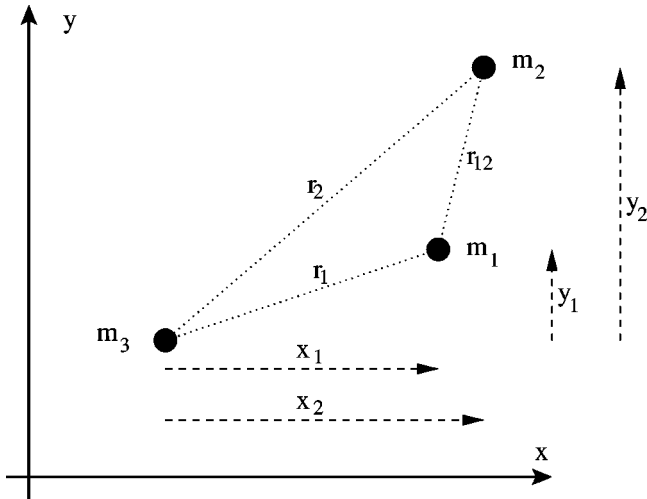


FIG. 1. The relative Cartesian coordinates of particles 1 and 2 with respect to particle 3 are  $(x_1, y_1)$  and  $(x_2, y_2)$ . The interparticle distances are  $r_1$ ,  $r_2$ , and  $r_{12}$ .

tions have been reported since the first one in 1993 [12–17], and compared with theoretical predictions [10,18]. In this context, a precise calculation of the energy levels of the excitonic trions in a 2D system as a function of the ratio of the effective masses, with and without external field, is highly valuable, and justifies the methods and calculations introduced in this paper. The 2D hydrogen molecular ion  $H_2^+$  has also been studied in the frame of the Born-Oppenheimer approximation in Ref. [19], where the first two electronic energy curves are given.

The paper is organized as follows. In Sec. II, we discuss the physical symmetries of the 2D three-body Coulomb problem. We then introduce a set of paraboliclike coordinates, give the expression of the Hamiltonian operator, and show that we can find a basis in which the Schrödinger equation involves sparse banded matrices, allowing accurate numerical calculations. In Sec. III, we analyze the group structure of the discrete symmetries of the Hamiltonian, showing that the complications introduced by the not one-to-one character of the change of coordinates can be taken into account exactly and actually do not lead to any difficulty. In Sec. IV, we first explain the detailed structure of the basis set that we use. We then discuss the structure of the expected energy spectrum in the case of a 2D helium atom with an infinite mass nucleus, and give the energies of the lowest levels in the bound Rydberg series, as well as—using the technique of complex coordinates—the energy and width of the first doubly excited resonance.

## II. THE SCHRÖDINGER EQUATION

### A. Hamiltonian

The three-body problem in two dimensions has six degrees of freedom that can be reduced to four in the center of mass frame. Here, as depicted in Fig. 1,  $\mathbf{r}_1$  and  $\mathbf{r}_2$  denote the positions of particle 1 and 2 with respect to particle 3, and  $\mathbf{p}_1$  and  $\mathbf{p}_2$  are the conjugate momenta. In atomic units (such that

$\hbar$ ,  $4\pi\epsilon_0$ , the mass  $m$  of the electron and the elementary charge are all equal to unity), the Hamiltonian is, neglecting QED and relativistic effects,

$$H = \frac{\mathbf{p}_1^2}{2\mu_{13}} + \frac{\mathbf{p}_2^2}{2\mu_{23}} + \frac{\mathbf{p}_1 \cdot \mathbf{p}_2}{m_3} + \frac{Q_1 Q_3}{r_1} + \frac{Q_2 Q_3}{r_2} + \frac{Q_1 Q_2}{r_{12}}, \quad (1)$$

where  $m_3$  is the mass of the third particle (in units of the electron mass), and  $\mu_{13}$  ( $\mu_{23}$ ) is the reduced mass of particle 1 (2) and particle 3.  $Q_1$ ,  $Q_2$ , and  $Q_3$  are the charges of the particles in units of the elementary charge.  $r_{12}$  is the distance between the particles 1 and 2. The 2D helium atom with a fixed nucleus corresponds to the case where  $m_3$  is infinite,  $\mu_{13} = \mu_{23} = 1$ ,  $Q_1 = Q_2 = -1$ , and  $Q_3 = 2$ .

As for the 3D three-body problem [20], we regularize the Schrödinger equation, i.e., remove the denominators, by multiplying it by  $16r_1 r_2 r_{12}$ . The eigenstate  $|\Psi\rangle$  with energy  $E$  then satisfies the generalized linear eigenequation

$$16r_1 r_2 r_{12} \left( \frac{\mathbf{p}_1^2}{2\mu_{13}} + \frac{\mathbf{p}_2^2}{2\mu_{23}} + \frac{\mathbf{p}_1 \cdot \mathbf{p}_2}{m_3} \right) |\Psi\rangle + V |\Psi\rangle = 16r_1 r_2 r_{12} E |\Psi\rangle, \quad (2)$$

where

$$V = 16(Q_1 Q_3 r_2 r_{12} + Q_2 Q_3 r_1 r_{12} + Q_1 Q_2 r_1 r_2). \quad (3)$$

### B. Symmetries

The symmetries of the 2D three-body problem are the rotational invariance around an axis ( $\Delta$ ) perpendicular to the plane, the parity  $\Pi$ , and, when particles 1 and 2 are identical, the exchange symmetry  $P_{12}$ . In two dimensions, the parity operator  $\Pi$  coincides with a rotation of angle  $\pi$  around  $\Delta$ , so that  $\Pi$  and the angular momentum  $L_z$  are related by

$$\Pi = (-1)^{L_z}. \quad (4)$$

We also introduce the two commuting symmetries  $\Pi_x$  (symmetry with respect to the  $x$  axis) and  $\Pi_y$  (symmetry with respect to the  $y$  axis). They are related to total parity through  $\Pi_x \Pi_y = \Pi_y \Pi_x = \Pi$ . The group generated by  $\Pi_x$ ,  $\Pi_y$ , and  $P_{12}$  is the so called  $D_{2h}$  point group. It is an invariance group of the Hamiltonian (1), for identical particles 1 and 2. The symmetries  $\Pi_x$  and  $\Pi_y$  both commute with parity, but not with the angular momentum, since, for instance,  $\Pi_x L_z = -L_z \Pi_x$ . As a consequence, the eigenstates of the 2D three-body Coulomb problem can be labeled by their angular momentum  $M_L = 0, \pm 1, \pm 2, \dots$  and by the exchange symmetry when particles 1 and 2 are identical. The spectrum corresponding to  $M_L$  and  $-M_L$  angular momenta are identical: this (Kramers) degeneracy is a direct consequence of the time reversal invariance of the problem [21]. Alternatively, the eigenstates could also be labeled by parity with respect to the  $x$  axis and the absolute value of the angular momentum.

When the system is exposed to an external uniform electric field along the  $x$  axis, the angular momentum is no longer preserved. The only remaining symmetries are  $\Pi_x$  and  $P_{12}$ .

### C. Parabolic coordinates

In order to perform efficient and accurate numerical calculations, we wish to obtain a sparse banded matrix representation of the linear problem (2) where the nonzero matrix elements are known in a closed form. We thus have to find a basis set in which the various terms of the Hamiltonian have strong selection rules. This can be achieved, for example, if all terms of the Hamiltonian can be expanded in polynomial combinations of position and (conjugate) momentum coordinates: in such a case, the set of eigenstates of a harmonic oscillator is convenient. Our situation is slightly more complicated, because the Hamiltonian involves the interparticle distance. How to deal with such a problem is well known for the hydrogen atom: by introducing a set of so-called parabolic or semiparabolic coordinates [22], one can map the 2D hydrogen atom on an harmonic oscillator. The method used here for the 2D helium atom is inspired by such a treatment, although it is technically more complicated.

If  $x$  and  $y$  are the Cartesian coordinates of a point in a 2D space and  $z = x + iy$  is the associated complex number, the distance from the origin is  $r = |z| = \sqrt{x^2 + y^2}$ , and its expression involves a square root function. The square root can be removed if we introduce the complex variable  $Z = X + iY$  defined by  $z = Z^2/2$ , since  $r = |Z|^2/2 = (X^2 + Y^2)/2$ .  $X$  and  $Y$  are the parabolic coordinates, related to  $x$  and  $y$  by

$$x = \frac{X^2 - Y^2}{2} \quad \text{and} \quad y = XY. \quad (5)$$

The parabolic coordinates are extremely convenient to represent the hydrogen atom in two dimensions [22], or the Stark effect of the 3D hydrogen atom [21]. Of course, the correspondence between  $(X, Y)$  and  $(x, y)$  given in Eq. (5) is not one to one. The difficulties related to that choice of coordinates are discussed in Sec. III B.

We now come to the case of three particles. The complex positions of particles 1 and 2 with respect to particle 3 are  $z_1$  and  $z_2$ , and  $Z_1$  and  $Z_2$  are the associated parabolic coordinates. The interparticle distances are then  $r_1 = |Z_1|^2/2$ ,  $r_2 = |Z_2|^2/2$ , and thus  $r_{12} = |z_1 - z_2| = |(Z_1 + Z_2)| |(Z_1 - Z_2)|/2$ . If we introduce the two complex numbers  $Z_p = (Z_1 + Z_2)/\sqrt{2}$  and  $Z_m = (Z_1 - Z_2)/\sqrt{2}$ , the distance  $r_{12}$  appears as the product of the moduli of  $Z_p$  and  $Z_m$ . Since we want to express  $r_{12}$  using square moduli, we introduce a second parabolic transformation on both  $Z_p$  and  $Z_m$  by setting  $Z_p = \Xi_p^2/2$  and  $Z_m = \Xi_m^2/2$ . The three distances are then expressed as the square moduli

$$r_1 = \frac{1}{16} |\Xi_p^2 + \Xi_m^2|^2, \quad (6)$$

$$r_2 = \frac{1}{16} |\Xi_p^2 - \Xi_m^2|^2, \quad (7)$$

$$r_{12} = \frac{1}{4} |\Xi_p \Xi_m|^2. \quad (8)$$

As a consequence, the three distances have polynomial expressions when they are expressed with the coordinates  $(x_p, y_p, x_m, y_m)$  defined by  $\Xi_p = x_p + iy_p$  and  $\Xi_m = x_m + iy_m$ . Those coordinates are related to the initial cartesian coordinates  $(x_1, y_1, x_2, y_2)$  by

$$\begin{aligned} x_1 &= \frac{1}{16} (x_p^2 - y_p^2 - 2x_p y_p + x_m^2 - y_m^2 - 2x_m y_m) \\ &\quad \times (x_p^2 - y_p^2 + 2x_p y_p + x_m^2 - y_m^2 + 2x_m y_m), \\ y_1 &= \frac{1}{4} (x_p^2 - y_p^2 + x_m^2 - y_m^2) (x_p y_p + x_m y_m), \\ x_2 &= \frac{1}{16} (x_p^2 - y_p^2 + 2x_p y_p - x_m^2 + y_m^2 - 2x_m y_m) \\ &\quad \times (x_p^2 - y_p^2 - 2x_p y_p - x_m^2 + y_m^2 + 2x_m y_m), \\ y_2 &= \frac{1}{4} (x_p^2 - y_p^2 - x_m^2 + y_m^2) (x_p y_p - x_m y_m), \end{aligned} \quad (9)$$

and the three distances are

$$\begin{aligned} r_1 &= \frac{1}{16} [(x_p - y_m)^2 + (y_p + x_m)^2] \\ &\quad \times [(x_p + y_m)^2 + (y_p - x_m)^2], \\ r_2 &= \frac{1}{16} [(x_p + x_m)^2 + (y_p + y_m)^2] \\ &\quad \times [(x_p - x_m)^2 + (y_p - y_m)^2], \\ r_{12} &= \frac{1}{4} (x_p^2 + y_p^2) (x_m^2 + y_m^2). \end{aligned} \quad (10)$$

### D. The Schrödinger equation

The Schrödinger equation (2) can be written as

$$\left\{ \frac{T_1}{2\mu_{13}} + \frac{T_2}{2\mu_{23}} + \frac{T_{12}}{m_3} + V \right\} |\Psi(x_p, y_p, x_m, y_m)\rangle = EB |\Psi(x_p, y_p, x_m, y_m)\rangle, \quad (11)$$

where the kinetic energy terms are

$$\begin{aligned}
 T_1 = & -\frac{1}{16}[(x_p+x_m)^2+(y_p+y_m)^2][(x_p-x_m)^2+(y_p-y_m)^2] \\
 & \times \left\{ (x_m^2+y_m^2)\left(\frac{\partial^2}{\partial x_p^2}+\frac{\partial^2}{\partial y_p^2}\right) + (x_p^2+y_p^2)\left(\frac{\partial^2}{\partial x_m^2}+\frac{\partial^2}{\partial y_m^2}\right) \right. \\
 & + 2(x_px_m+y_py_m)\left(\frac{\partial^2}{\partial x_p\partial x_m}+\frac{\partial^2}{\partial y_p\partial y_m}\right) - 2(x_py_m \\
 & \left. - y_px_m)\left(\frac{\partial^2}{\partial x_p\partial y_m}-\frac{\partial^2}{\partial y_p\partial x_m}\right) \right\}, \\
 T_2 = & -\frac{1}{16}[(x_p-y_m)^2+(y_p+x_m)^2][(x_p+y_m)^2+(y_p-x_m)^2] \\
 & \times \left\{ (x_m^2+y_m^2)\left(\frac{\partial^2}{\partial x_p^2}+\frac{\partial^2}{\partial y_p^2}\right) + (x_p^2+y_p^2)\left(\frac{\partial^2}{\partial x_m^2}+\frac{\partial^2}{\partial y_m^2}\right) \right. \\
 & - 2(x_px_m+y_py_m)\left(\frac{\partial^2}{\partial x_p\partial x_m}+\frac{\partial^2}{\partial y_p\partial y_m}\right) \\
 & \left. + 2(x_py_m-y_px_m)\left(\frac{\partial^2}{\partial x_p\partial y_m}-\frac{\partial^2}{\partial y_p\partial x_m}\right) \right\}, \\
 T_{12} = & -\frac{1}{16}[(x_p^2+y_p^2)^2-(x_m^2+y_m^2)^2]\left\{ (x_m^2+y_m^2)\left(\frac{\partial^2}{\partial x_p^2}+\frac{\partial^2}{\partial y_p^2}\right) \right. \\
 & \left. - (x_p^2+y_p^2)\left(\frac{\partial^2}{\partial x_m^2}+\frac{\partial^2}{\partial y_m^2}\right) \right\} - \frac{1}{2}(x_px_m+y_py_m) \\
 & \times (x_py_m-y_px_m)\left\{ (x_px_m+y_py_m)\left(\frac{\partial^2}{\partial y_p\partial x_m}-\frac{\partial^2}{\partial x_p\partial y_m}\right) \right. \\
 & \left. - (x_py_m-y_px_m)\left(\frac{\partial^2}{\partial x_p\partial x_m}+\frac{\partial^2}{\partial y_p\partial y_m}\right) \right\}, \\
 B = & 16r_1r_2r_{12}. \tag{12}
 \end{aligned}$$

The expressions of  $B$  and  $V$  can be deduced from Eqs. (3) and (10). The Jacobian of the coordinate transformation is  $16r_1r_2r_{12}$ . The scalar product of the two wave functions is given in Appendix B.

The various terms in the Schrödinger equation (11) are polynomials in the coordinates  $(x_p, y_p, x_m, y_m)$  and their associated momenta (partial derivatives  $-i\partial/\partial\{x_p, y_p, x_m, y_m\}$ ). The operators  $T_1, T_2, T_{12}, V$ , and  $B$  can thus be expressed using the corresponding annihilation and creation operators:

$$a_{x_p} = \frac{1}{\sqrt{2}}\left(x_p + \frac{\partial}{\partial x_p}\right), \quad a_{x_p}^\dagger = \frac{1}{\sqrt{2}}\left(x_p - \frac{\partial}{\partial x_p}\right). \tag{13}$$

This shows that the 2D three-body Coulomb problem can be described using the annihilation and creation operators of four harmonic oscillators. The Hamiltonian is a polynomial of degree 12 in the annihilation and creation operators. Con-

sequently, it will be possible to choose a basis of tensorial products of Fock states of each harmonic oscillator, for which the operators involved in the Schrödinger equation exhibit strong coupling rules.

From the annihilation and creation operators associated with the new coordinates, we introduce the right and left circular operators in the planes  $(x_p, y_p)$  and  $(x_m, y_m)$  defined by

$$\begin{aligned}
 a_1 &= (a_{x_p} - ia_{y_p})/\sqrt{2}, \\
 a_2 &= (a_{x_p} + ia_{y_p})/\sqrt{2}, \\
 a_3 &= (a_{x_m} - ia_{y_m})/\sqrt{2}, \\
 a_4 &= (a_{x_m} + ia_{y_m})/\sqrt{2}. \tag{14}
 \end{aligned}$$

Using the symbolic calculation language MAPLE V, we have calculated the normal ordered expression of the various operators involved in the Hamiltonian. Those expressions are too long to be published here. Indeed, the operators  $T_1$  and  $T_2$  contain 625 terms,  $T_{12}$  331, the potential operators  $r_1r_{12}$  and  $r_2r_{12}$  517,  $r_1r_2$  159, and  $B$  1463. When particles 1 and 2 are identical, the Hamiltonian involves the kinetic term  $T_1 + T_2$  and the potential term  $(r_1+r_2)r_{12}$  that have only 335 and 275 terms, because the terms of  $T_1$  and  $T_2$  that do not commute with the exchange operator  $P_{12}$  cancel out.

### E. Angular momentum

The angular momentum  $L_z$  has a very simple expression when expressed with the  $(x_p, y_p, x_m, y_m)$  coordinates:

$$\begin{aligned}
 L_z = & -i\left(x_1\frac{\partial}{\partial y_1}-y_1\frac{\partial}{\partial x_1}+x_2\frac{\partial}{\partial y_2}-y_2\frac{\partial}{\partial x_2}\right), \\
 L_z = & -\frac{i}{4}\left(x_p\frac{\partial}{\partial y_p}-y_p\frac{\partial}{\partial x_p}+x_m\frac{\partial}{\partial y_m}-y_m\frac{\partial}{\partial x_m}\right). \tag{15}
 \end{aligned}$$

The relation  $z=Z^2/2$  between the cartesian and parabolic complex numbers shows that a rotation of angle  $\theta$  in  $Z$  is a rotation of  $2\theta$  in  $z$ . Consequently, a factor of 2 appears in the expression of the angular momentum in parabolic coordinates [22]. Since we have performed two successive parabolic transformations to define the  $(x_p, y_p, x_m, y_m)$  coordinates, we have a factor of 4 in the denominator of Eq. (15). With the annihilation and creation operators (14), the angular momentum is simply

$$L_z = (N_1 - N_2 + N_3 - N_4)/4, \tag{16}$$

where the number operators are  $N_i = a_i^\dagger a_i$ . They are related to the number operators corresponding to the annihilation and creation operators  $a_{x_p}, \dots$  given in Eq. (13) by

$$\begin{aligned}
 N_1 + N_2 &= N_{x_p} + N_{y_p}, \\
 N_3 + N_4 &= N_{x_m} + N_{y_m}.
 \end{aligned}
 \tag{17}$$

### III. DISCRETE SYMMETRIES

#### A. Physical symmetries

The Hamiltonian (1) has two discrete symmetries,  $\Pi_x$  and  $\Pi_y$ , which are the symmetries with respect to two orthogonal axis in the physical plane. Using the  $(x_p, y_p, x_m, y_m)$  coordinates, they can be expressed, for instance, as

$$\begin{aligned}
 \Pi_x : x_p &\rightarrow x_p, & \Pi_y : x_p &\rightarrow (x_p + y_p)/\sqrt{2}, \\
 y_p &\rightarrow -y_p, & y_p &\rightarrow (x_p - y_p)/\sqrt{2}, \\
 x_m &\rightarrow x_m, & x_m &\rightarrow (x_m + y_m)/\sqrt{2}, \\
 y_m &\rightarrow y_m, & y_m &\rightarrow (x_m - y_m)/\sqrt{2}.
 \end{aligned}
 \tag{18}$$

Moreover, if particles 1 and 2 are identical, the Hamiltonian commutes with the exchange operator  $P_{12}$ . The effect of  $P_{12}$  on the  $(x_p, y_p, x_m, y_m)$  coordinates is

$$\begin{aligned}
 P_{12} : x_p &\rightarrow x_p, \\
 y_p &\rightarrow y_p, \\
 x_m &\rightarrow y_m, \\
 y_m &\rightarrow -x_m.
 \end{aligned}
 \tag{19}$$

Obviously, the Schrödinger equation (11) written with the  $(x_p, y_p, x_m, y_m)$  coordinates is invariant under these transformations.

#### B. “Additional” symmetries

In this section, we analyze the constraints that the physical wave functions must satisfy. We first recall what happens in the case of a single parabolic transformation. The parabolic transformation  $(X, Y) \rightarrow (x, y)$  defined in Eq. (5) is a one-to-one mapping of the quarter of plane  $(X \geq 0, Y \geq 0)$  onto the half plane  $(x, y \geq 0)$ . Here, the transformation is used to represent the full Cartesian plane  $(x, y)$  by extending the domains of  $X$  and  $Y$  to  $]-\infty, +\infty[$ . In that way, we obtain a double mapping of the Cartesian plane since  $(X, Y)$  and  $(-X, -Y)$  are mapped on the same point. Consequently, the Hamiltonian written with the parabolic coordinates has a new discrete symmetry  $(X, Y) \rightarrow (-X, -Y)$ , i.e., the parity with respect to  $(X, Y)$ . The physical wave function must be a single-valued function of the initial coordinates  $(x, y)$ , i.e., must satisfy  $\Psi(X, Y) = \Psi(-X, -Y)$ . Any function of  $\Psi(X, Y)$  that satisfies the Schrödinger equation written in the  $(X, Y)$  coordinates but does not obey the constraint  $\Psi(X, Y) = \Psi(-X, -Y)$  is to be rejected as an unphysical solution.

In the particular case where the wave function is expanded on a basis built with tensorial products of harmonic oscillator eigenstates,

$$|\Psi\rangle = \sum_{n_X, n_Y} C_{n_X, n_Y} |n_X\rangle \otimes |n_Y\rangle,
 \tag{20}$$

the physical wave function expansion of Eq. (20) is restricted to the even values of  $n_X + n_Y$ , because the parity of the Fock state  $|n\rangle$  is  $(-1)^n$  [22].

This property can be extended to the case of the transformation given in Eq. (9) that gives the Cartesian coordinates versus the coordinates  $(x_p, y_p, x_m, y_m)$ . Because we perform four parabolic transformations to obtain the  $(x_p, y_p, x_m, y_m)$  coordinates from the initial Cartesian coordinates, there are four “additional” discrete symmetries which leave the Schrödinger equation (11) invariant. We denote them by  $\Pi_1$  defined as  $(X_1, Y_1) \rightarrow (-X_1, -Y_1)$ ,  $\Pi_2$ ,  $\Pi_p$ , and  $\Pi_m$ . The effects of those symmetries on the  $(x_p, y_p, x_m, y_m)$  coordinates are

$$\begin{aligned}
 \Pi_1 : x_p &\rightarrow -y_m, & \Pi_2 : x_p &\rightarrow x_m, \\
 y_p &\rightarrow x_m, & y_p &\rightarrow y_m, \\
 x_m &\rightarrow -y_p, & x_m &\rightarrow x_p, \\
 y_m &\rightarrow x_p, & y_m &\rightarrow y_p, \\
 \Pi_p : x_p &\rightarrow -x_p, & \Pi_m : x_p &\rightarrow x_p, \\
 y_p &\rightarrow -y_p, & y_p &\rightarrow y_p, \\
 x_m &\rightarrow x_m, & x_m &\rightarrow -x_m, \\
 y_m &\rightarrow y_m, & y_m &\rightarrow -y_m.
 \end{aligned}
 \tag{21}$$

#### C. Symmetries of the wave function

The group  $G$  generated by the  $\Pi_x, \Pi_y, P_{12}$  and the  $\Pi_1, \Pi_2, \Pi_p, \Pi_m$  symmetries is an invariance group of the Schrödinger equation (11). It is studied in details and its character table is given in Appendix A.

In order to be single valued in the geometrical space  $(x_1, y_1, x_2, y_2)$ , the wave function  $\Psi(x_p, y_p, x_m, y_m)$  must be invariant under any “additional” symmetry introduced by the non one-to-one change of coordinates, i.e., under any of the transformations  $\Pi_1, \Pi_2, \Pi_p, \Pi_m$ . Then, the wave function must belong to an irreducible representation of  $G$  for which the character of any “additional” symmetry is equal to its dimension. There are only eight representations with this property, all being one dimensional, that correspond to the first eight lines of the character table given in Appendix A. Consequently, the physical eigenfunctions  $\Psi(x_p, y_p, x_m, y_m)$  can be distinguished only by their symmetry properties with respect to  $\Pi_x, \Pi_y$ , and  $P_{12}$ . The eight physical irreducible representations of  $G$  are those of the group  $D_{2h}$  (or  $mmm$ ), of order 8, already mentioned in Sec. II B. The application that maps each “additional” symmetry on the identity is a group homomorphic mapping of  $G$  on  $D_{2h}$ .

Finally, we have shown here that all energy levels belong to a one-dimensional representation of the discrete symmetry group of the Schrödinger equation, and are thus expected to be nondegenerate [except for the  $(M_L, -M_L)$  mentioned above]. Moreover, using the  $(x_p, y_p, x_m, y_m)$  coordinates does not introduce extra representations which cannot be distinguished from the physical ones. The wave functions can be described using a basis exhibiting the relevant symmetry properties with respect to  $\Pi_x$ ,  $\Pi_y$ , and  $P_{12}$ , or  $L_z$  and  $P_{12}$ . The second feature will be extensively used in the numerical implementation.

In other words, among all solutions of the Schrödinger equation (11) in the  $(x_p, y_p, x_m, y_m)$  coordinates, sorting out the unphysical solutions is rather straightforward and one is left only with the physical symmetries of the initial system.

#### IV. NUMERICAL SOLUTION

##### A. Basis set

###### 1. Basis structure

To perform numerical calculations of the eigenenergies and eigenstates of the three-body Coulomb problem, we expand the Schrödinger equation on a convenient basis, and then solve a linear eigenvalue problem. Because the different terms of the Hamiltonian have polynomial expressions in the annihilation and creation operators, we obtain strong selection rules if we choose basis functions that are tensorial products of Fock states  $|n_i\rangle$  of the harmonic oscillator described by the circular annihilation operator  $a_i$ , namely, we set

$$|n_1, n_2, n_3, n_4\rangle = |n_1\rangle \otimes |n_2\rangle \otimes |n_3\rangle \otimes |n_4\rangle. \quad (22)$$

The indices  $n_i$  are then positive integers. The basis functions are eigenfunctions of the angular momentum, corresponding to the integer eigenvalue

$$M_L = (n_1 - n_2 + n_3 - n_4)/4. \quad (23)$$

The wave functions of these basis states are simple. Indeed, they are just eigenstates of a harmonic oscillator along the various coordinates. In the  $(x_p, y_p, x_m, y_m)$  coordinates, they should appear as products of Hermite polynomials and Gaussian functions of the coordinates. As we use circular creation-annihilation operators, Eq. (14), the associated eigenstates of the two-dimensional harmonic oscillators in the  $(x_p, y_p)$  and  $(x_m, y_m)$  planes are easily written in polar coordinates as the product of an  $\exp(i\phi)$  term with an exponential and a Laguerre polynomial of the squared radius. The explicit expressions of such states can be found in [22].

We have previously shown that the two successive parabolic transformations introduce “additional” unphysical states. The physical solutions can be selected using a basis set that is even with respect to all the “additional” symmetries. This choice is performed in two steps. First, both  $n_1 + n_2$  and  $n_3 + n_4$  have to be even numbers. Indeed, from Eq. (17),  $n_1 + n_2 = n_{x_p} + n_{y_p}$  and  $n_3 + n_4 = n_{x_m} + n_{y_m}$  and the even representations for  $\Pi_p$  and  $\Pi_m$  correspond to even values of  $n_{x_p} + n_{y_p}$  and  $n_{x_m} + n_{y_m}$ . Secondly, because the transformation  $(1,2,3,4) \rightarrow (3,4,1,2)$  on the annihilation and creation op-

erators commutes with the Hamiltonian and corresponds to the identity in physical space, the basis functions have to be chosen as the symmetric combinations:

$$|n_1, n_2, n_3, n_4\rangle^+ = |n_1, n_2, n_3, n_4\rangle + |n_3, n_4, n_1, n_2\rangle. \quad (24)$$

Of course, this symmetrized state remains an eigenstate of the angular momentum, with the same eigenvalue  $M_L$ . Taking into account the even parity of  $n_1 + n_2$  and  $n_3 + n_4$ , and thus of  $n_1 - n_2$  and  $n_3 - n_4$ , and the expression of  $M_L$ , we obtain that  $n_1 - n_2 \pmod{4}$  and  $n_3 - n_4 \pmod{4}$  are simultaneously equal to either 0 or 2. We then set

$$C_{12} = (n_1 - n_2) \pmod{4} = (n_3 - n_4) \pmod{4}. \quad (25)$$

When particles 1 and 2 are identical, the Hilbert space can be split into a singlet subspace corresponding to  $C_{12}=0$ , and a triplet subspace corresponding to  $C_{12}=2$ . Here, singlet means symmetric with respect to the exchange operator  $P_{12}$  whereas triplet means antisymmetric.

We can now define precisely the basis set corresponding to the physical states with angular momentum  $M_L$  and either singlet or triplet exchange symmetry. Since the quadruplet of indices  $(n_1, n_2, n_3, n_4)$  and  $(n_3, n_4, n_1, n_2)$  give the same symmetrized ket in Eq. (24), we have only to consider one of the two quadruplets to uniquely label the symmetrized basis. Consequently, for singlet states, we set

$$\begin{aligned} \mathcal{B}_{M_L}^{\text{sym}} = \{ & |n_1, n_2, n_3, n_4\rangle^+, n_1 - n_2 + n_3 - n_4 = 4M_L, n_i \geq 0, \\ & C_{12} = 0, (n_1 > n_3 \text{ or } (n_1 = n_3 \text{ and } n_2 \geq n_4)) \}, \end{aligned} \quad (26)$$

and for triplet states

$$\begin{aligned} \mathcal{B}_{M_L}^{\text{anti sym}} = \{ & |n_1, n_2, n_3, n_4\rangle^+, n_1 - n_2 + n_3 - n_4 = 4M_L, n_i \geq 0, \\ & C_{12} = 2, (n_1 > n_3 \text{ or } (n_1 = n_3 \text{ and } n_2 > n_4)) \}. \end{aligned} \quad (27)$$

###### 2. Selection rules and matrix elements

Two basis vectors  $|n_1, n_2, n_3, n_4\rangle$  and  $|n_1 + \delta n_1, n_2 + \delta n_2, n_3 + \delta n_3, n_4 + \delta n_4\rangle$  are coupled by the Hamiltonian if the shifts  $\delta n_i$  correspond to one of the 225 allowed coupling rules. Because the Hamiltonian commutes with the total angular momentum, they all obey  $\delta n_1 - \delta n_2 + \delta n_3 - \delta n_4 = 0$ . Among them, 159 rules preserve the exchange symmetry while 66 do not. The 159 rules that appear for the operators  $T_1 + T_2$ ,  $T_{12}$ ,  $(r_1 + r_2)r_{12}$ ,  $r_1 r_2$ , and  $B$  obey  $\delta n_1 - \delta n_2 = -(\delta n_3 - \delta n_4) = 0$  or  $\delta n_1 - \delta n_2 = -(\delta n_3 - \delta n_4) = \pm 4$ , and are shown in Fig. 2. The 66 rules verify  $\delta n_1 - \delta n_2 = -(\delta n_3 - \delta n_4) = \pm 2$ . They appear if the exchange symmetry is broken ( $m_1 \neq m_2$  or  $Q_1 \neq Q_2$ ) in the kinetic terms  $T_1, T_2$ , and the potential terms  $r_1 r_{12}$  and  $r_2 r_{12}$ .

Since the Hamiltonian has been written in normal order, the derivation of the matrix elements is straightforward. They are too numerous to be written explicitly here [30]. We only give two matrix elements of the kinetic operator of the

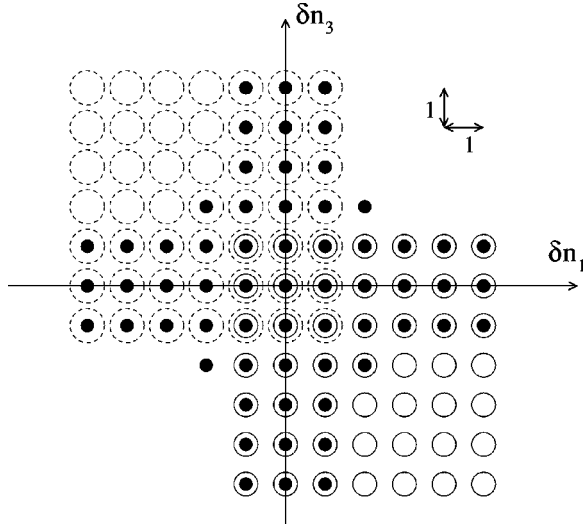


FIG. 2. The 159 selection rules that preserve the exchange symmetry are depicted in the  $(n_1, n_3)$  space. The dark circles correspond to the 61 rules  $\delta n_1 = \delta n_2$  and  $\delta n_3 = \delta n_4$ , the full line circles to the 49 rules  $\delta n_1 - \delta n_2 = 4$  and  $\delta n_3 - \delta n_4 = -4$ , and the dashed line circles to the 49 rules  $\delta n_1 - \delta n_2 = -4$  and  $\delta n_3 - \delta n_4 = 4$ .

2D helium  $T_1 + T_2$  between two unsymmetrized basis vectors:

$$\begin{aligned} \langle n_1, n_2, n_3, n_4 | (T_1 + T_2) | n_1, n_2, n_3, n_4 \rangle \\ = (1/4)(n_1 + n_2 + 1)(n_3 + n_4 + 1)(n_1^2 + 4n_1n_2 - n_1n_3 \\ + n_1n_4 + n_2^2 + n_2n_3 - n_2n_4 + n_3^2 + 4n_3n_4 + n_4^2 + 3n_1 \\ + 3n_2 + 3n_3 + 3n_4 + 8), \end{aligned} \quad (28)$$

as well as the matrix element corresponding to the selection rule  $\delta_1 = \delta_2 = \delta_3 = \delta_4 = 1$ :

$$\begin{aligned} \langle n_1 + 1, n_2 + 1, n_3 + 1, n_4 + 1 | (T_1 + T_2) | n_1, n_2, n_3, n_4 \rangle \\ = -(1/4)\sqrt{n_4 + 1}\sqrt{n_3 + 1}\sqrt{n_2 + 1}\sqrt{n_1 + 1}(n_1^2 + 5n_1n_2 \\ - 2n_1n_4 + n_2^2 - 2n_2n_3 + n_3^2 + 5n_3n_4 + n_4^2 + 5n_1 + 5n_2 \\ + 5n_3 + 5n_4 + 12). \end{aligned} \quad (29)$$

### 3. Numerical implementation

For the numerical calculations, we have chosen to truncate the basis defined by Eq. (26) or (27) using the condition  $n_1 + n_2 + n_3 + n_4 \leq N_{base}$ . Because the angular momentum is fixed, we have only three independent indices, and the size of the basis is roughly  $N_{base}^3/192$ . The basis  $\mathcal{B}$  is then ordered in order to represent the Schrödinger equation using band matrices as narrow as possible. The eigenvalue problem is then solved using the Lanczos algorithm [23] which makes it possible to compute a few eigenvalues in the range of interest.

### 4. Variational parameter

So far, the natural length scale of the problem is the Bohr radius  $a_0$ . Because it is not necessarily the best suited one, we introduce the length scale  $\alpha^{-1/4}a_0$ . The Schrödinger equation (11) is written

$$\begin{aligned} \left\{ \alpha^4 \left( \frac{T_1}{2\mu_{13}} + \frac{T_2}{2\mu_{23}} + \frac{T_{12}}{m_3} \right) + \alpha^8 V \right\} |\Psi\rangle \\ = \alpha^{12} EB |\Psi\rangle. \end{aligned} \quad (30)$$

When the basis is truncated, the length scale  $\alpha$  becomes a variational parameter (i.e., the calculated energy levels should not depend on  $\alpha$  if the basis set is large enough) that has to be numerically optimized. All the numerical results presented in this paper are obtained with  $\alpha$  close to 0.4. All the digits of the energy levels given in the tables are significant. The uncertainty on the results is thus 1 on the last figure, and the relative accuracy reaches the  $10^{-13}$  level.

### B. The 2D helium atom without electron interaction

Let us consider 2D helium with a fixed nucleus of charge  $Q_3 = 2$  (the mass  $m_3$  is infinite). The Schrödinger equation (30) is simply

$$\left\{ \alpha^4 \frac{T_1 + T_2}{2} + \alpha^8 V \right\} |\Psi\rangle = \alpha^{12} EB |\Psi\rangle, \quad (31)$$

where  $V = -32(r_1 + r_2)r_{12} + 16r_1r_2$ . If the  $16r_1r_2$  term in the potential energy is removed, the three-body problem corresponds to two independent 2D hydrogen atoms with a nucleus of charge  $Q = 2$ . The spectrum of the 2D hydrogen atom is well known, and is given by the series [22]:

$$E_{N,M} = -\frac{Q^2}{2(N-1/2)^2}, \quad (32)$$

where  $N \geq 1$  is the principal quantum number and  $-N+1 \leq M \leq N-1$  the angular momentum of the electron; the degeneracy is  $2N-1$ . The structure of the energy spectrum is very similar to the 3D energy spectrum, the only difference being that the effective quantum number  $N-1/2$  is a half integer ranging from  $1/2$  to infinity rather than a non-negative integer.

For the helium atom without electronic interaction, the spectrum is thus given by

$$E_{N_1, M_1} + E_{N_2, M_2} = -\frac{4}{2(N_1-1/2)^2} - \frac{4}{2(N_2-1/2)^2}, \quad (33)$$

where  $N_1$  and  $N_2$  are the principal quantum numbers of the two electrons. The essential degeneracy is  $2(2N_1-1)(2N_2-1)$  if  $N_1 \neq N_2$  and  $(2N_1-1)^2$  otherwise [31]. The total angular momentum is simply given by  $M_L = M_1 + M_2$ . The states of total angular momentum  $M_L$  correspond to the indices  $(N_1, M_1, N_2, M_2)$  and  $(N_2, M_2, N_1, M_1)$ . Those degenerate states give symmetric (singlet) and antisymmetric (trip-

let) states when the two quadruplets are different and only one symmetric state if they are equal. Finally, the energy levels can be labeled by  $N_1$ ,  $N_2$ ,  $M_L$ , and  $P_{12}$ . The degeneracy of this configuration is given by the number of solutions of  $M_L = M_1 + M_2$  taking into account the boundaries on  $M_1$  and  $M_2$ .

By solving the Schrödinger equation for an angular momentum between  $-3$  and  $3$ , and for the two exchange symmetries, we have checked that our method gives the expected eigenenergies and degeneracies.

We have then checked the effect of the electronic interaction by introducing it perturbatively as  $\epsilon/r_{12}$ . We have numerically computed the ground state energy of the three-body problem as a function of  $\epsilon$  and observed a linear behavior, as expected from first-order perturbation theory. The slope in atomic units is  $4.70(1)$ , in agreement with the slope  $3\pi/2$  predicted by first-order perturbation theory (see Appendix B).

### C. The 2D helium atom

The  $1/r_{12}$  term describing the electronic repulsion is now taken into account. This does not affect the positions of the various ionization thresholds (as the electron interaction vanishes at large distance). There is an infinite number of single-ionization thresholds associated with the principal quantum number of the hydrogenic state of the resulting  $\text{He}^+$  ion, given by energies

$$I_N = -\frac{4}{2(N-1/2)^2}. \quad (34)$$

These single-ionization thresholds form a series that converges to the double-ionization threshold at zero energy.

Consequently, one expects bound states below energy  $I_1 = -8$  a.u., resonance (doubly excited states) between  $I_1$  and zero, and only continua above.

#### 1. Bound states

The lowest energy levels of the 2D helium below the first ionization limit are given in Table I for the singlet states and in Table II for the triplet states. For each value of  $M_L$ , we obtain a Rydberg series converging to the  $N=1$  threshold. For such excited states, the outer electron lies far from the nucleus while the inner electron is essentially in its ground state and lies very close to the nucleus. Because this picture gives two very different roles to the two electrons, it results in a different set of quantum numbers, namely,  $(N, M)$  for the inner electron and  $(n, m)$  for the outer one. A brutal but useful approximation is to neglect the effect of the outer electron on the inner one, i.e., consider the inner electron in the hydrogenic state  $N=1, M=0$  while the outer electron experiences a point charge  $Q=1$  (the charge  $+2$  of the nucleus screened by the charge  $-1$  of the inner electron) at the origin, resulting in an energy spectrum  $-8 - 1/[2(n-1/2)^2]$ , where  $n$  is the principal quantum number of the (hydrogenic) outer electron. This is of course only an ap-

TABLE I. Energy levels of the singlet states of the 2D helium atom (with infinite mass of the nucleus), below the first ionization threshold. The optimum variational parameter  $\alpha$  is close to 0.4. For most of the states, the basis truncation is given by  $N_{base}=200$ . The basis size is then 43 626 for singlet  $M_L=0$  states, and slightly decreases with  $M_L$ . For  $(1,0,4,0)$ ,  $(1,0,5,0)$ , and  $(1,0,6,0)$  we use  $N_{base}=240$  and a basis size of 74 801. In the fourth column,  $\delta_{n,m}$  is the quantum defect of the state, as deduced from Eq. (35).

$N, M, n, m$	$M_L$	Energy (a.u.)	$\delta_{n,m}$
1,0,1,0	0	-11.899 822 342 953	0.1419
1,0,2,0	0	-8.250 463 875 379	0.0871
1,0,3,0	0	-8.085 842 792 777	0.0866
1,0,4,0	0	-8.042 911 011 139	0.0865
1,0,5,0	0	-8.025 668 309 76	0.0864
1,0,6,0	0	-8.017 061 08	0.0864
1,0,2,1	1	-8.211 542 089 886	-0.0374
1,0,3,1	1	-8.077 637 328 985	-0.0378
1,0,4,1	1	-8.039 947 878	-0.0378
1,0,5,1	1	-8.024 280 94	-0.0379
1,0,3,2	2	-8.079 805 619 119	-0.0030
1,0,4,2	2	-8.040 745 817	-0.0030
1,0,5,2	2	-8.024 657 76	-0.0031
1,0,6,2	2	-8.016 51	-0.0031
1,0,7,2	2	-8.011 80	

proximation. Deviations from it can be measured through the quantum defect  $\delta_{n,m}$  defined directly from the energy levels through

$$E_{1,0,n,m} = -8 - \frac{1}{2(n-1/2-\delta_{n,m})}. \quad (35)$$

If the previous approximation were exact, the quantum defects would all be zero. Hence, deviations from zero and

TABLE II. Energies of the triplet states of the 2D helium atom (with infinite mass of the nucleus), below the first ionization threshold. The optimum variational parameter  $\alpha$  is close to 0.4. The basis truncation is given by  $N_{base}=200$ . The basis size is 43 550 for triplet  $M_L=0$  states. In the fourth column,  $\delta_{n,m}$  is the quantum defect of the state, as deduced from Eq. (35).

$N, M, n, m$	$M_L$	Energy (a.u.)	$\delta_{n,m}$
1,0,2,0	0	-8.295 963 728 090	0.2002
1,0,3,0	0	-8.094 583 618 582	0.2008
1,0,4,0	0	-8.045 941 305 572	0.2010
1,0,5,0	0	-8.027 055 169	0.2011
1,0,6,0	0	-8.017 807	0.2011
1,0,2,1	1	-8.225 772 173 259	0.0118
1,0,3,1	1	-8.080 919 691 737	0.0142
1,0,4,1	1	-8.041 165 882 92	0.0149
1,0,5,1	1	-8.024 858 500	0.0152
1,0,3,2	2	-8.079 819 688 304	-0.0028
1,0,4,2	2	-8.040 751 693 48	-0.0028
1,0,5,2	2	-8.024 661 158	-0.0028
1,0,6,2	2	-8.016 512	-0.0028

TABLE III. Quantum defects for various series of the 2D and 3D helium atoms below the first ionization threshold. The values in the 3D case are calculated from the energies given in [24]. The values in the 2D case are the limits of  $\delta_{n,m}$  for large values of  $n$ .

3D Rydberg series		2D Rydberg series	
	$\delta$	$N, M_L$	$\delta$
$^1S^e$	0.140	1,0	0.0864
$^3S^e$	0.299	1,0	0.2011
$^1P^o$	-0.012	1,1	-0.0379
$^3P^o$	0.068	1,1	0.0152
$^1D^e$	0.0021	1,2	-0.0031
$^3D^e$	0.0028	1,2	-0.0028

evolutions with  $n$  and  $m$  directly measure the breaking of the approximation. The results shown in Tables I and II show that—as for the 3D helium atom—the quantum defects in a given series tend to a constant value as  $n \rightarrow \infty$ . When  $|m|$  is increased, the outer electron is repelled from the nucleus by the centrifugal energy barrier and fills less the area occupied by the inner electron. It is thus expected that the quantum defects will decrease with increasing  $|m|$  and this is fully confirmed by our “exact” diagonalizations, (see Tables I, II, and III). Also, in the triplet states, the wave function in configuration space is antisymmetric, so that the two electrons cannot be at the same place. Consequently, they are less efficiently affected by each other, resulting in a lower interaction energy and consequently a larger quantum defect. Again, our “exact” calculations confirm this behavior.

Finally, it is interesting to compare the 2D and 3D situations. Although the Rydberg series are similar in both cases, this is not true for the ground state. Indeed, the binding energy of the inner electron in its ground state is 8 a.u., [see Eq. (32)], in 2D, that is, four times more than in the 3D helium atom. Almost the same ratio 4 is observed between the total binding energies of the ground state: 11.90 a.u. in 2D versus 2.91 a.u. in 3D.

For singly excited states, the core is also four times smaller in 2D. We then expect a smaller core penetration because the centrifugal barrier is almost the same in the 2D and 3D systems, and also a smaller core polarization by the outer electron, resulting in smaller quantum defects in the 2D case. The comparison of the 2D and the 3D quantum defects in Table III is consistent with this interpretation.

## 2. Resonances

Above the first ionization threshold, the spectrum contains resonances embedded into the continuum. They can be numerically separated using the complex rotation method [25,26] (also known as the method of complex coordinates), where the positions and momenta  $\mathbf{r}$  and  $\mathbf{p}$  are respectively changed into  $\mathbf{r}e^{i\theta}$  and  $\mathbf{p}e^{-i\theta}$ . Here, it is simply implemented using a complex length scale  $\alpha = |\alpha|e^{i\theta}$  (in order to preserve their canonical commutation relations). This results in a “complex rotated” non-Hermitian Hamiltonian whose eigenvalues are complex. In the complex energy plane, the resonances do not depend on the angle  $\theta$  while the continua are

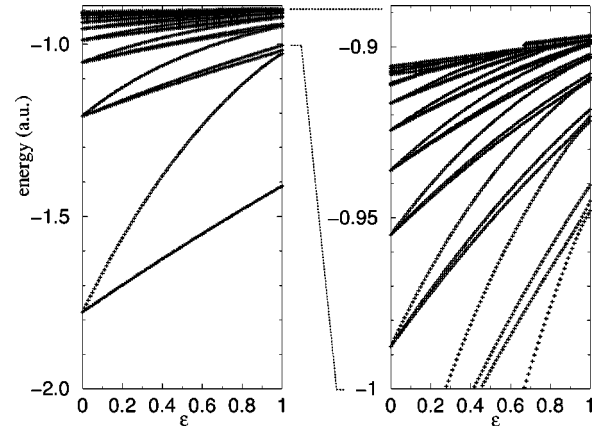


FIG. 3. Energy levels of the singlet  $M_L=0$  resonances of the 2D helium atom (nucleus with infinite mass) between the first ( $-8$  a.u.) and the second ( $-0.888 \dots$  a.u.) ionization thresholds as a function of the magnitude  $\epsilon$  of the electronic interaction included in the potential energy as  $\epsilon/r_{12}$ . The right part of the figure is a magnification close to the second ionization threshold. All the energies presented in this picture are well converged and obtained with  $\alpha=0.5$ ,  $\theta=0.12$ , and  $N_{base}=150$ . The basis size is 18 696. Because the method of complex coordinates is used, these energy levels are not bound states, but resonances. At the scale of this figure, their widths are very small.

rotated by an angle of  $2\theta$  around the ionization thresholds. The first resonance of the 2D helium atom (infinite mass of the nucleus) is obtained for zero angular momentum and singlet exchange symmetry. Its energy is

$$E = -1.411\,496\,328(1) - i0.001\,241\,734(1) \text{ a.u.} \quad (36)$$

It is obtained for a rotation angle  $\theta \approx 0.4$ , a length scale  $\alpha \approx 0.35$ ,  $N_{base} = 150$ , and a basis size of 18 696.

The energy structure of the resonances is illustrated in the case of the singlet  $M_L=0$  states in Fig. 3. The electronic repulsion is included in the potential energy as  $\epsilon/r_{12}$  with  $0 \leq \epsilon \leq 1$ . One can follow the energy levels as a function of  $\epsilon$  from the independent electron case ( $\epsilon=0$ ) to the helium case ( $\epsilon=1$ ). For  $\epsilon=0$ , the levels correspond to the Rydberg series  $N=2$ ,  $n \geq 2$  converging to  $I_2 = -8/9$  a.u. The degeneracy of the ( $N=2, n=2$ ) configuration is 9, with three states of zero total angular momentum. Two of them have the singlet symmetry and one the triplet symmetry. For  $n > 2$ , the degeneracy of the configuration is 18, with six states corresponding to  $M_L=0$  (three singlet and three triplet states). Consequently, for  $\epsilon=0$ , the first  $M_L=0$  singlet resonance is doubly degenerate, and the following ones are triply degenerate. The introduction of the electronic interaction removes the degeneracy.

## D. The 2D $H^-$ ion

The  $H^-$  ion with a fixed nucleus is obtained by setting  $Q_3=1$ . We obtain only one bound state below the first ionization limit [at  $-2$  a.u. from Eq. (32)], with zero angular momentum and singlet exchange symmetry. Its energy is

$$E = -2.240\,275\,363\,589(1) \text{ a.u.} \quad (37)$$

It is obtained for  $\alpha \approx 0.4$ ,  $N_{base} = 220$ , the basis size being 57 820.

## V. CONCLUSION

We have introduced a different set of coordinates to represent the 2D three-body Coulomb problem and given the resulting Schrödinger equation. We have discussed the discrete symmetry group properties of the equation and shown that it can be numerically solved very efficiently, using a convenient basis set for which the Schrödinger equation involves sparse banded matrices. The convergence of the calculations is very good and the numerical results are extremely accurate. This is demonstrated in the case of the 2D helium atom (with infinite mass of the nucleus), for which the lowest energy levels in the bound Rydberg series are given with a relative accuracy in the  $10^{-9}$  to  $10^{-13}$  range.

The method developed in this paper provides an efficient tool for studying the dynamics of the 2D helium atom in an external electric field aligned along the  $x$  axis. Indeed, with a field of strength  $F$ , we must add the external potential energy term  $V_{ext} = 16r_1r_2r_{12}(x_1+x_2)F$  to Eq. (3). The only remaining symmetries are then the exchange symmetry  $P_{12}$  and the symmetry with respect to the  $x$  Cartesian axis  $\Pi_x$ . In such a case, the convenient basis set can be defined, from Eq. (24), by

$$|n_1, n_2, n_3, n_4\rangle^\epsilon = |n_1, n_2, n_3, n_4\rangle^+ + \epsilon |n_2, n_1, n_4, n_3\rangle^+, \quad (38)$$

with  $\epsilon = \pm 1$  for even or odd states with respect to  $\Pi_x$ . Because  $V_{ext}$  is a polynomial in these coordinates, it exhibits selection rules, making an accurate diagonalization of the Schrödinger equation still possible.

The motion of the nucleus can easily be taken into account, including the  $T_{12}$  contribution to the Hamiltonian in Eq. (11). In that way, it will be possible to determine very accurately the ground state energy of excitonic trions, as a function of the electron to hole mass ratio. This work is in progress.

## ACKNOWLEDGMENTS

Laboratoire Kastler Brossel de l'Université Pierre et Marie Curie et de l'École Normale Supérieure is UMR 8552 du CNRS. CPU time on various computers has been provided by IDRIS. The authors acknowledge Monique Combescot for stimulating discussions on the trion problem.

## APPENDIX A: CHARACTER TABLE

The discrete symmetry group  $G$  of the Schrödinger equation (11) written in the  $(x_p, y_p, x_m, y_m)$  coordinates is studied here. It is generated by the  $\Pi_x, \Pi_y, P_{12}$  physical symmetries and the  $\Pi_1, \Pi_2, \Pi_p, \Pi_m$  "additional" symmetries, defined in Eqs. (18), (19), and (21). Its structure has been studied following standard methods of the theory of finite groups (see, for example, [27,28]). Because all the generators of the

group can be seen as a permutation among the 16 quantities  $x_p, y_p, x_m, y_m, (x_p + y_p)/\sqrt{2}, (x_p - y_p)/\sqrt{2}, (x_m + y_m)/\sqrt{2}, (x_m - y_m)/\sqrt{2}$  and the opposite values, the  $G$  group appears as a subgroup of the permutation group of 16 elements. Because of this property, it is easily studied using the permutation group package provided by the MAPLE language.

The group  $G$  contains 128 elements, in 29 classes. It has 16 one-dimensional, eight two-dimensional, and five four-dimensional irreducible representations. Table IV represents its complete character table. It has been obtained using the method described in [28]. Let the classes of  $G$  be  $K_i$  with  $1 \leq i \leq n$ . The set  $K_i K_j$ , the set of the products of any element of the class  $K_i$  by any element of the class  $K_j$ , is made of complete classes. Calling  $c_{ijl}$  the number of occurrences of the class  $K_l$  in the product  $K_i K_j$ , one can symbolically write

$$K_i K_j = \sum_l c_{ijl} K_l. \quad (A1)$$

This property is used to obtain relations between characters  $\chi_i^{(R)}$  of the class  $K_i$  in an irreducible representation  $R$ :

$$g_i g_j \chi_i^{(R)} \chi_j^{(R)} = \chi_E^{(R)} \sum_{l=1}^{29} c_{ijl} g_l \chi_l^{(R)}, \quad (A2)$$

where  $g_i$  is the number of elements of the class  $K_i$  and  $\chi_E^{(R)}$  is the character of the identity  $E$ , i.e., the dimension of the representation  $R$ . The  $n$  characters of an irreducible representation appear to be the solutions of the  $n(n+1)/2$  quadratic equations obtained from Eq. (A2) for any couple of  $(i, j)$ . Then, to construct the character table of the group, three steps are necessary. First, the group has to be separated into classes, and the number  $g_i$  are obtained. Second, the numbers  $c_{ijl}$  are computed, and last the system of equations (A2) is solved. Obviously, there are  $n$  different sets of solutions, corresponding to the  $n$  irreducible representations.

## APPENDIX B: SCALAR PRODUCT

The scalar product of two wave functions  $|\Psi^{(1)}\rangle$  and  $|\Psi^{(2)}\rangle$  in the  $(x_p, y_p, x_m, y_m)$  coordinates is

$$\begin{aligned} \langle \Psi^{(1)} | \Psi^{(2)} \rangle &= \frac{1}{16} \int \int \int \int \Psi^{(1)}(x_p, y_p, x_m, y_m) * B \Psi^{(2)} \\ &\times (x_p, y_p, x_m, y_m) dx_p dy_p dx_m dy_m, \end{aligned} \quad (B1)$$

where  $B$  is given by Eq. (12). The integrals are calculated from  $-\infty$  to  $+\infty$ . The factor  $1/16 = 1/2^4$  comes from the four double mappings of the space introduced by the change to parabolic coordinates.

We now calculate the average value of  $1/r_{12}$  for the ground state  $|\Psi_{0,0}\rangle$  of a 2D helium atom without electronic repulsion, that is

TABLE IV. Character table of the discrete symmetry group G of the Schrödinger equation (11). The classes and the irreducible representations have been organized in order to obtain the character table of the  $D_{2h}$  group in the upper left corner (in bold figures). The last three classes are those of the “additional” symmetries  $\Pi_2$ ,  $\Pi_1$ , and  $\Pi_p$  ( $\Pi_p$  and  $\Pi_m$  belong to the same class). The first line gives the number of elements in each class. We finally give one element of each of the 29 classes: E,  $\Pi_y$ ,  $\Pi_x$ ,  $\Pi_y\Pi_x$ ,  $P_{12}$ ,  $\Pi_yP_{12}$ ,  $\Pi_xP_{12}$ ,  $\Pi_y\Pi_xP_{12}$ ,  $\Pi_p\Pi_m$ ,  $\Pi_2\Pi_x\Pi_m$ ,  $\Pi_2P_{12}$ ,  $\Pi_1\Pi_2$ ,  $\Pi_2\Pi_xP_{12}$ ,  $\Pi_p\Pi_y\Pi_xP_{12}$ ,  $\Pi_pP_{12}$ ,  $\Pi_2\Pi_x$ ,  $\Pi_2\Pi_y$ ,  $\Pi_2\Pi_y\Pi_x$ ,  $\Pi_1\Pi_2\Pi_m$ ,  $\Pi_2\Pi_y\Pi_m$ ,  $\Pi_2\Pi_y\Pi_xP_{12}$ ,  $\Pi_2\Pi_yP_{12}$ ,  $\Pi_y\Pi_x\Pi_m$ ,  $\Pi_p\Pi_y\Pi_x\Pi_m$ ,  $\Pi_1\Pi_y\Pi_xP_{12}$ ,  $\Pi_y\Pi_xP_{12}^{-1}$ ,  $\Pi_2$ ,  $\Pi_1$ ,  $\Pi_p$ ; some of them are reported in the second line of the table.

1	8	8	2	4	8	8	4	1	4	8	2	8	2	4	4	4	8	2	4	4	8	4	2	4	2	4	4	2	
E	$\Pi_y$	$\Pi_x$	$\Pi_y\Pi_x$	$P_{12}$	$\Pi_yP_{12}$	$\Pi_xP_{12}$	$\Pi_y\Pi_xP_{12}$																			$\Pi_2$	$\Pi_1$	$\Pi_p$	
																											$\Pi_m$		
<b>1</b>	<b>1</b>	<b>1</b>	<b>1</b>	<b>1</b>	<b>1</b>	<b>1</b>	<b>1</b>	<b>1</b>	1	1	1	1	1	1	1	1	1	1	1	1	1	1	1	1	1	1	1	1	
<b>1</b>	<b>-1</b>	<b>1</b>	<b>-1</b>	<b>1</b>	<b>-1</b>	<b>1</b>	<b>1</b>	<b>-1</b>	1	1	1	1	1	-1	1	1	-1	-1	1	-1	-1	-1	-1	-1	-1	-1	-1	-1	
<b>1</b>	<b>1</b>	<b>-1</b>	<b>-1</b>	<b>1</b>	<b>1</b>	<b>1</b>	<b>-1</b>	<b>-1</b>	1	-1	1	1	-1	-1	1	-1	1	1	-1	1	-1	1	-1	-1	-1	-1	1	1	
<b>1</b>	<b>-1</b>	<b>-1</b>	<b>1</b>	<b>1</b>	<b>-1</b>	<b>-1</b>	<b>-1</b>	<b>1</b>	1	1	-1	1	1	-1	1	-1	1	1	-1	1	-1	1	-1	1	1	1	1	1	
<b>1</b>	<b>1</b>	<b>1</b>	<b>1</b>	<b>-1</b>	<b>-1</b>	<b>-1</b>	<b>-1</b>	<b>-1</b>	1	1	-1	1	-1	-1	1	-1	1	1	-1	-1	1	-1	1	1	-1	-1	1	1	
<b>1</b>	<b>-1</b>	<b>1</b>	<b>-1</b>	<b>-1</b>	<b>1</b>	<b>-1</b>	<b>-1</b>	<b>1</b>	1	1	1	-1	1	-1	-1	1	-1	1	1	-1	-1	1	-1	-1	-1	1	1	1	
<b>1</b>	<b>1</b>	<b>-1</b>	<b>-1</b>	<b>-1</b>	<b>-1</b>	<b>-1</b>	<b>1</b>	<b>1</b>	1	1	-1	-1	1	1	-1	-1	1	1	1	-1	-1	1	-1	-1	-1	1	1	1	
<b>1</b>	<b>-1</b>	<b>-1</b>	<b>1</b>	<b>-1</b>	<b>1</b>	<b>1</b>	<b>1</b>	<b>-1</b>	1	-1	-1	-1	1	1	-1	-1	1	1	-1	-1	1	1	-1	-1	-1	1	1	1	
1	1	1	1	1	1	1	1	1	1	1	-1	-1	1	-1	-1	1	-1	-1	-1	1	1	-1	-1	1	1	1	-1	1	
1	-1	1	-1	1	-1	1	1	-1	-1	1	-1	-1	1	1	1	1	1	1	1	-1	-1	1	-1	-1	-1	-1	-1	1	
1	1	-1	-1	1	1	1	-1	-1	-1	1	1	-1	1	1	-1	1	1	-1	-1	-1	-1	-1	-1	-1	-1	-1	-1	1	
1	-1	-1	1	1	-1	-1	-1	1	1	1	1	-1	1	1	-1	1	1	-1	1	1	1	1	1	1	1	-1	-1	1	
1	1	1	1	-1	-1	-1	-1	-1	-1	1	-1	-1	1	1	1	1	-1	-1	-1	-1	-1	-1	-1	-1	-1	-1	-1	1	
1	-1	1	-1	-1	1	-1	-1	1	1	1	-1	1	1	1	1	1	-1	-1	-1	-1	-1	-1	-1	-1	-1	-1	-1	1	
1	1	-1	-1	-1	-1	-1	1	-1	1	1	1	1	1	-1	1	1	-1	-1	-1	-1	-1	-1	-1	-1	-1	-1	-1	1	
2	0	0	-2	0	0	0	0	0	2	2	0	2	0	0	0	-2	2	0	-2	-2	0	0	2	-2	0	0	0	-2	
2	0	0	2	0	0	0	0	0	2	2	0	2	0	0	0	-2	-2	0	-2	2	0	0	-2	2	0	0	0	-2	
2	0	0	2	0	0	0	0	0	2	-2	0	2	0	0	0	2	2	0	-2	-2	0	0	-2	2	0	0	0	-2	
2	0	0	-2	0	0	0	0	0	2	-2	0	2	0	0	0	-2	-2	0	-2	2	0	0	2	-2	0	0	0	-2	
2	0	0	0	0	0	0	0	-2	2	0	0	-2	0	2	0	0	0	2	0	-2	0	0	0	0	0	2	2	-2	
2	0	0	0	0	0	0	0	2	2	0	0	-2	0	-2	0	0	0	0	2	0	2	0	0	0	0	-2	-2	-2	
2	0	0	0	0	0	0	0	2	2	0	0	-2	0	-2	0	0	0	0	2	0	-2	0	0	0	0	2	-2	-2	
4	0	0	0	0	0	0	0	0	4	0	0	-4	0	0	0	0	0	0	0	0	0	0	0	0	0	0	0	4	
4	0	0	$-\sqrt{8}$	2	0	0	0	0	-4	0	0	0	0	$\sqrt{8}$	-2	0	0	0	0	0	0	0	0	0	$\sqrt{8}$	0	$-\sqrt{8}$	0	0
4	0	0	$\sqrt{8}$	-2	0	0	0	0	-4	0	0	0	0	$\sqrt{8}$	2	0	0	0	0	0	0	0	0	0	$-\sqrt{8}$	0	$-\sqrt{8}$	0	0
4	0	0	$\sqrt{8}$	2	0	0	0	0	-4	0	0	0	0	$-\sqrt{8}$	-2	0	0	0	0	0	0	0	0	0	$-\sqrt{8}$	0	$\sqrt{8}$	0	0
4	0	0	$-\sqrt{8}$	-2	0	0	0	0	-4	0	0	0	0	$-\sqrt{8}$	2	0	0	0	0	0	0	0	0	0	$\sqrt{8}$	0	$\sqrt{8}$	0	0

$$\sigma = \left\langle \Psi_{0,0} \left| \frac{1}{r_{12}} \right| \Psi_{0,0} \right\rangle. \tag{B2}$$

We now evaluate  $\sigma$  using the  $(x_p, y_p, x_m, y_m)$  coordinates. Since the Jacobian of the coordinate transformation is  $B = 16r_1r_2r_{12}$ ,  $\sigma$  becomes

The normalized wave function of the ground state of a 2D hydrogenic atom with a nucleus of charge  $Q$  is

$$\Psi_0(r_1) = \sqrt{\frac{2}{\pi}} Q e^{-2Qr_1}, \tag{B3}$$

$$\sigma = \int \int \int \int 16r_1r_2 |\Psi_{0,0}(x_p, y_p, x_m, y_m)|^2 \times dx_p dy_p dx_m dy_m, \tag{B5}$$

so that

$$\Psi_{0,0}(r_1, r_2) = \Psi_{0,0}(r_1) \Psi_{0,0}(r_2) = \frac{8Q^2}{\pi} e^{-2Q(r_1+r_2)}. \tag{B4}$$

where  $r_1$  and  $r_2$  are given by Eqs. (10). The integrals are calculated from  $-\infty$  to  $+\infty$ .

To evaluate  $\sigma$ , we represent the  $(x_p, y_p)$  and  $(x_m, y_m)$  planes using polar coordinates  $(r_p, \theta_p)$  and  $(r_m, \theta_m)$  and obtain from Eq. (10)

$$\begin{aligned} r_1 &= \frac{1}{16} [r_p^4 + r_m^4 + 2r_p^2 r_m^2 \cos(2\theta_p - 2\theta_m)], \\ r_2 &= \frac{1}{16} [r_p^4 + r_m^4 - 2r_p^2 r_m^2 \cos(2\theta_p - 2\theta_m)], \\ r_{12} &= \frac{r_p^2 r_m^2}{4}. \end{aligned} \quad (\text{B6})$$

The ground state wave function is then

$$\Psi_{0,0}(r_p, \theta_p, r_m, \theta_m) = \frac{8Q^2}{\pi} e^{-Q(r_p^4 + r_m^4)/2}, \quad (\text{B7})$$

so that

$$\begin{aligned} \sigma &= \frac{Q^4}{4\pi^2} \int \int \int \int \{r_p^8 + r_m^8 + 2r_p^4 r_m^4 \\ &\times [1 - 2\cos^2(2\theta_p - 2\theta_m)]\} e^{-Q(r_p^4 + r_m^4)/2} \\ &\times r_p dr_p r_m dr_m d\theta_p d\theta_m. \end{aligned} \quad (\text{B8})$$

The integration over  $\theta_p$  and  $\theta_m$  gives 0 for the angular dependent term and  $4\pi^2$  for the independent one. The integration over  $r_p$  and  $r_m$  involves Gaussian integrals that give

$$\sigma = \frac{3\pi Q}{4}, \quad (\text{B9})$$

which is  $3\pi/2$  when  $Q=2$ . In the 3D case,  $\sigma$  is evaluated to  $5Q/8$  in [29]. The ratio  $\sigma_{2D}/\sigma_{3D} = 6\pi/5 \approx 3.77$  is close to 4, because the 2D ground state wave function is four times smaller than the 3D wave function.

- 
- [1] G. Tanner, K. Richter, and J.-M. Rost, *Rev. Mod. Phys.* **72**, 497 (2000).
- [2] R. Püttner, B. Grémaud, D. Delande, M. Domke, M. Martins, A. S. Schlachter, and G. Kaindl, *Phys. Rev. Lett.* **86**, 3747 (2000).
- [3] A. Bürgers, D. Wintgen, and J.-M. Rost, *J. Phys. B* **28**, 3163 (1995).
- [4] S. P. Goldman, *Phys. Rev. A* **57**, R677 (1998).
- [5] G. W. F. Drake, *Phys. Scr. T* **83**, 83 (1999).
- [6] V. I. Korobov, *Phys. Rev. A* **61**, 064503 (2000).
- [7] O. Chuluunbaatar, I. V. Puzynin, and S. I. Vinitisky, *J. Phys. B* **34**, 425 (2001).
- [8] B. Eckhardt and K. Sacha, *Europhys. Lett.* **56**, 651 (2001).
- [9] M. A. Lampert, *Phys. Rev. Lett.* **1**, 450 (1958).
- [10] B. Stébé and A. Ainane, *Superlattices Microstruct.* **5**, 545 (1989).
- [11] A. I. Bobrysheva, M. V. Grodetskii, and V. T. Zyukov, *J. Phys. C* **16**, 5723 (1983).
- [12] K. Kheng, R. T. Cox, Y. Merle d'Aubigné, F. Bassani, K. Saminadayar, and S. Tatarenko, *Phys. Rev. Lett.* **71**, 1752 (1993).
- [13] G. Finkelstein, H. Shtrikman, and I. Bar-Joseph, *Phys. Rev. Lett.* **74**, 976 (1995).
- [14] H. Buhmann, L. Mansouri, J. Wang, P. H. Beton, N. Mori, L. Eaves, M. Henini, and M. Potemski, *Phys. Rev. B* **51**, 7969 (1995).
- [15] A. J. Shields, M. Pepper, D. A. Ritchie, M. Y. Simmons, and G. A. C. Jones, *Phys. Rev. B* **51**, 18049 (1995).
- [16] N. Paganotto, J. Siviniant, D. Coquillat, D. Scalbert, J.-P. Lascaray, and A. V. Kavokin, *Phys. Rev. B* **58**, 4082 (1998).
- [17] V. Huard, R. T. Cox, K. Saminadayar, A. Arnoult, and S. Tatarenko, *Phys. Rev. Lett.* **84**, 187 (2000).
- [18] D. M. Whittaker and A. J. Shields, *Phys. Rev. B* **56**, 15185 (1997).
- [19] J.-L. Zhu and J.-J. Xiong, *Phys. Rev. B* **41**, 12274 (1990).
- [20] K. Richter, J. S. Briggs, D. Wintgen, and E. A. Solov'ev, *J. Phys. B* **25**, 3929 (1992).
- [21] L. Landau and E. Lifchitz, *Quantum Mechanics* (MIR, Moscow, 1966).
- [22] M. J. Englefield, *Group Theory and the Coulomb Problem* (Wiley, New York, 1972).
- [23] T. Ericsson and A. Ruhe, *Math. Comput.* **35**, 1251 (1980), and references therein.
- [24] F. S. Levin and D. A. Micha, *Long Range Casimir Forces, Theory, and Recent Experiment on Atomic Systems* (Plenum, London, 1993).
- [25] Y. K. Ho, *Phys. Rev. A* **44**, 4154 (1991).
- [26] E. Balslev and J. M. Combes, *Commun. Math. Phys.* **22**, 280 (1971).
- [27] M. Petrachene and E. Trifonov, *Applications de la Théorie des Groupes à la Mécanique Quantique* (Masson, Paris, 1970).
- [28] M. Hamermesh, *Group Theory and its Application to Physical Problems* (Dover, New York, 1989); see, for instance, Secs. 3.17 and 4.2.
- [29] H. A. Bethe and E. E. Salpeter, *Quantum Mechanics of One and Two Electron Atoms* (Springer-Verlag, Berlin, 1957), see Eqs. (33.4) and (33.6).
- [30] An alternative method for computing matrix elements is to use the explicit expressions of the basis state wave functions, and compute the action of the various operators using well-known recursion relations between Laguerre polynomials. The algebraic method that we use is much safer.
- [31] Accidental degeneracies may occur for particular couples of principal quantum numbers.